Front. Environ. Sci. Eng. 2015, 9(5): 832–839
DOI 10.1007/s11783-015-0778-x

RESEARCH ARTICLE

Removing polybrominated diphenyl ethers in pure water using Fe/Pd bimetallic nanoparticles

Min ZHANG[1], Jian LU (✉)[2], Zhencheng XU (✉)[3], Yiliang HE[1], Bo ZHANG[1], Song JIN[4], Brian BOMAN[2]

1 School of Environmental Science and Engineering, Shanghai Jiao Tong University, Shanghai 200240, China
2 Indian River Research and Education Center, University of Florida, Fort Pierce, FL 34945, USA
3 South China Institute of Environment Sciences, Ministry of Environmental Protection, Guangzhou 510655, China
4 Department of Civil and Architectural Engineering, University of Wyoming, Laramie, WY 82071, USA

Abstract Polybrominated diphenyl ethers (PBDEs) have been widely used as fire-retardants. Due to their high production volume, widespread usage, and environmental persistence, PBDEs have become ubiquitous contaminants in various environments.Nanoscale zero-valent iron (ZVI) is an effective reductant for many halogenated organic compounds. To enhance the degradation efficiency, ZVI/Palladium bimetallic nanoparticles (nZVI/Pd) were synthesized in this study to degrade decabromodiphenyl ether (BDE209) in water. Approximately 90% of BDE209 was rapidly removed by nZVI/Pd within 80 min, whereas about 25% of BDE209 was removed by nZVI. Degradation of BDE209 by nZVI/Pd fits pseudo-first-order kinetics. An increase in pH led to sharply decrease the rate of BDE209 degradation. The degradation rate constant in the treatment with initial pH at 9.0 was more than 6.8 × higher than that under pH 5.0. The degradation intermediates of BDE209 by nZVI/Pd were identified and the degradation pathways were hypothesized. Results from this study suggest that nZVI/Pd may be an effective tool for treating polybrominated diphenyl ethers (PBDEs) in water.

Keywords bimetallic nanoparticles, nanoscale zero-valent iron, polybrominated diphenyl ethers, degradation

1 Introduction

Polybrominated diphenyl ethers (PBDEs) are types of fire-retardants that have been produced since early 1960s [1]. PBDEs have been known to cause neuro toxins and have been identified as endocrine disruptors [2]. PBDEs have been found in various environmental and biologic samples including birds, edible marine organisms, marine mammals, and human beings [3,4]. These halogenated organic contaminants are hydrophobic (less water soluble) and recalcitrant [5,6], and consequently, their concentrations in the environment and foods increase over time [7].

Among commercially available PBDEs, decabromodiphenyl ether (BDE209) is the only one currently produced in large quantities worldwide [8]. BDE209 (water solubility $< 0.1\ \mu g \cdot L^{-1}$) is less water soluble, but it is highly soluble in organic solvents such as tetrahydrofuran (THF) and acetone [9,10]. For this reason, most studies have focused on removal of BDE209 in the presence of organic solvents [9,10]. However, limited information is available for the fate of BDE209 and other PBDEs in natural water systems. Moreover, the use of organic solvents in most studies compromise the practical development of techniques for treating PBDEs in waters.

Surface area and reactivity of conventional zero-valent iron (ZVI) particles increase significantly when particle size is reduced to 10–100 nm [11]. Nanoscale zero-valent iron (nZVI) has been used as an effective reductant for treating many halogenated organic compounds including TCE, PCBs, and PBDEs [11–15]. However, nZVI alone was not effective for removing PBDEs [10]. Iron (Fe)-based bimetallic nanoparticles have been tested to degrade PBDEs in the presence of organic solvents [9,16–18]. In such systems, catalytic hydrogenation was proposed as the major pathway for the debromination of PBDEs [19]. Since water could provide protons more quickly than organic co-solvents such as methanol, the degradation efficiency was usually inhibited by organic co-solvents [20–22].

In this study, the feasibility of using nZVI/Pd to remove BDE209 in water was investigated. The kinetics of BDE209 transformation in water under different pH

Received September 7, 2014; accepted February 23, 2015

E-mail: lujian.leonard@gmail.com, xuzhencheng@scies.org

conditions and degradation pathways were also investigated.

2 Materials and methods

2.1 Chemical and reagents

BDE209 (purity > 98%) was purchased from TCI (Tokyo, Japan). A standard mixture of 39 PBDEs and individual standards BDE205, 206, 209 were purchased from Accustandard (New Haven, USA) and used to analyze degradation intermediates. Solutions used for high-performance liquid chromatography (HPLC) and experimental setups such as methanol, acetonitrile, THF, $FeSO_4 \cdot 7H_2O$, $NaBH_4$, and K_2PdC1_6 were purchased from Merk (Darmstadt, Germany) and Sinopharm (Shanghai, China). Milli-Q double distilled water was used throughout the study. Granular iron (300 μm, specific surface area 2.7 $m^2 \cdot g^{-1}$) was obtained from Edmund Scientific Co. (Tonawanda, USA).

2.2 Preparation of BDE209 water solution

BDE209 water solution was prepared by following a solvent exchange protocol. BDE209 was first dissolved in THF, and then added into water drop-by-drop. During the dilution process, the BDE209/THF was fully spread and well dispersed through vigorous stirring under room temperature. At the end of the dilution process, the residual THF was removed through a quick distillation. After the evaporation, 100 mL of BDE209 water solution was placed in a stirred cell (Model 8200, Millipore, Billerica, USA) with ultrafiltration membrane (YM10, molecular weight cut-off = 10000, Millipore, Billerica, USA). Fifty (50) mL of pure water was added when the volume of original BDE209 solution decreased to 50 mL. This washing process was repeated 12 times. Finally, BDE209 water solution were filtered by microporous filtering film (d = 0.22 μm). Concentration of BDE209 in the stock water solution was made to be 10 $mg \cdot L^{-1}$.

2.3 Preparation of Fe/Pd bimetallic nanoparticles

The Fe/Pd bimetallic nanoparticles (nZVI/Pd) were synthesized using the sodium borohydride ($NaBH_4$) reduction method [15,16]. $FeSO_4 \cdot 7H_2O$ was dissolved into a 30:70 methanol/deionized water (v/v) solution, and NaOH solution was added to the dissolved iron solution to yield a pH of 6.1. $NaBH_4$ (1.3 $mol \cdot L^{-1}$) solution was then rapidly added to the $FeSO_4 \cdot 7H_2O$ solution. The resulting particle suspension was centrifuged to remove the excess $NaBH_4$. The nZVI was rinsed three times with deoxygenated water and ethanol. To make Fe/Pd-coated bimetallic nanoparticles, a specified amount of K_2PdC1_6 solution was added into nZVI. The mixture was stirred for 40 min. Separation and washing procedures were similar to that of nZVI. Finally, both nZVI/Pd and nZVI/Pd nanoparticles were dried in a vacuum at 50°C overnight.

2.4 Characterization of Fe/Pd bimetallic nanoparticles and BDE209 in pure water

Particle size was determined by using particle size and zeta potential analyzer (ZS 90, Malvern Instruments Ltd., UK). The content (wt.%) of Pd in nZVI/Pd was determined using inductively coupled plasma optical emission spectrometer (iCAP6300,Thermo Electron, Waltham, USA). The surface area of the particles was analyzed by surface area and porosimetry analyzer (ASAP 2010 M + C, Micromeritics Inc., Norcross, USA). THF in the PBDE 209 water solution was analyzed using HPLC methods.

2.5 Removal of BDE209 using Fe/Pd bimetallic nanoparticles

Batch experiments were conducted to evaluate debromination of BDE209 using bimetallic nanoparticles (nZVI/Pd) particles. The stock solution of BDE209 was first diluted to 2 $mg \cdot L^{-1}$ using a gentle stream of nitrogen water. The diluted stock solution of BDE209 (1.5 mL) was added into serum vials (1.5 mL) before 0.01 g of nZVI/Pd particles was added. Each bottle was covered with a Teflonlined cap and incubated at 30°C on a rotary shaker (125 $r \cdot min^{-1}$). The pH of the nZVI-Pd solution was 5.0. Triplicates were set up for all experiments. Treatments containing no nZVI/Pd served as the control. Parallel experiments were also performed with microscale iron (0.01 g) and nZVI (0.01 g). To evaluate the effect of pH on the degradation of BDE209 in the presence of nZVI/Pd, the initial pHs of the treatments were set to 5.0, 7.0, 8.0, and 9.0 using HCl (0.1 $mol \cdot L^{-1}$) or NaOH (0.1 $mol \cdot L^{-1}$), as needed.

2.6 Analytical method

THF in the BDE209 water solution was analyzed using a LC-2010 series HPLC with a Shimadzu C18 column (4.6 mm i.d. × 250 mm) and an isocratic eluent (95% acetonitrile and 5% water) at a flow rate of 1.0 mL $\cdot min^{-1}$. At scheduled time intervals, serum vials were removed from the rotary shaker. The mixture in the serum vial was transformed into a 15 mL glass tube before being subjected to liquid–liquid extraction with a 3-fold volume of dichloromethane. The mixture was vortexed for 3 min and shaken for 1 h under room temperature. Through the extraction procedure, PBDEs residuals in both water and on the surface of remedial agent (nZVI/Pd, nZVI, or microscale iron) were all extracted into dichloromethane. The extract was transferred to gas chromatography (GC) vial for analysis.

BDE209 and its degradation intermediates were detected using a GCMS-QP2010 GC coupled to a mass

spectrometer operated in negative chemical ionization (NCI) mode. A DB-5HT (15 m × 0.25 mm × 0.1 mm) capillary column was used with helium as the carrier gas at a constant flow rate of 1.5 mL·min^{-1}. The inlet temperature was held at 320°C. The oven temperature program was as follows: initial temperature 100°C, hold for 3.5 min; increased to 320°C at 20°C·min^{-1}; hold at 320°C for 6 min. The ion source temperature was 250°C. A sample volume of 1 μL was injected in splitless mode. The mass spectrometer was in selected ion monitoring (SIM) mode at $m/z = 79 + 81$.

The purchased standard mixture of PBDEs were also separated on the gas chromatography–mass spectrometry (GC-MS) for debromination byproduct identification of *non*-BDE (BDE206), *hepta*-BDEs, *hexa*-BDEs, *penta*-BDEs, *tetra*-BDEs, and *tri*-BDEs. Unidentified PBDEs can be presumptively identified by comparing relative retention time and order with those reported in the retention studies of *non*-BDEs including BDE207 and BDE208 [9,23], and *octa*-BDEs [24–27]. For BDE209 quantitative analysis, the method detection limit (MDL) was 0.01 μg·L^{-1} and the method recovery was greater than 80%.

A pseudo-first-order kinetic model was applied to describe degradation of BDE209 [19]. Observed degradation rate constants (k_{obs}) were calculated according to the following expressions:

$$\ln\frac{[A]_0}{[A]_t} = k_{obs}t, (\text{first order reaction}) \quad (1)$$

where $[A]_0$ and $[A]_t$ refer to BDE209 concentrations at the beginning and end time t when samples were collected, respectively.

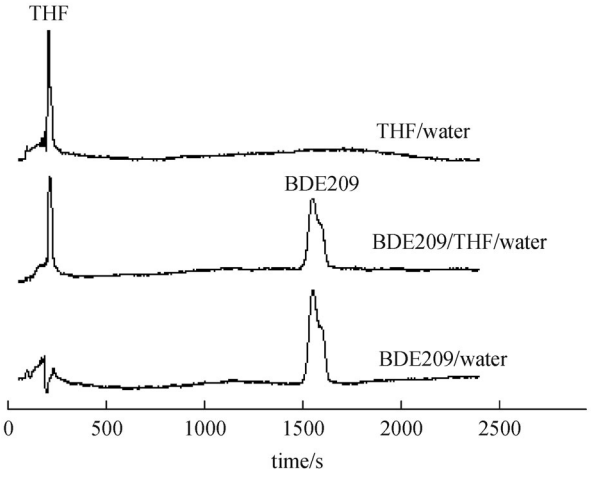

Fig. 1 HPLC chromatogram of THF/water, BDE209/THF/water, and BDE209/water. The peak at 3.6 min refers to THF

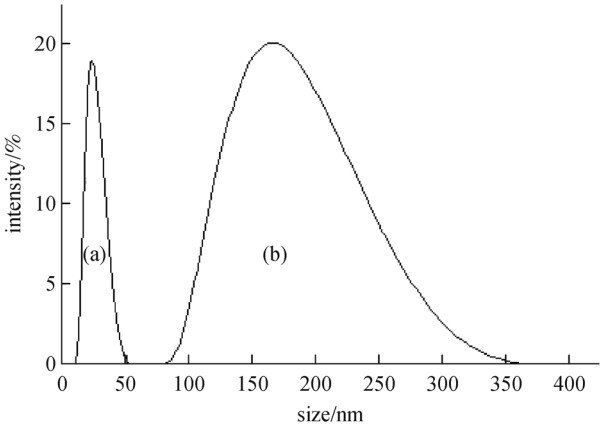

Fig. 2 The particle size distribution of nano-BDE209 aggregates (a) and Fe/Pd bimetallic nanoparticles (b)

3 Results

3.1 Characterization of BDE209 in pure water solution and Fe/Pd bimetallic nanoparticles

The residual THF in water was shown in Fig. 1. There was no THF peak at 3.6 min in the pure-water system, indicating that THF has been successfully removed from water in the BDE209/water system. The particle size of BDE209 in water was characterized (Fig. 2(a)). The results indicate that BDE209 were nano-scale particles in the solution, with particle size distribution ranging from 122 nm to 220 nm, and a mean diameter of 164 nm.

The nZVI/Pd particles synthesized in this study had a grain size ranging from 18 nm to 53 nm, with a mean diameter of 26 nm as measured by DLS (Fig. 2(b)). The percentage weight of Pd in the particle of the nZVI/Pd was 0.32%. The surface area of nZVI was 31.1 m^2·g^{-1} compared to 43.4 m^2·g^{-1} for nZVI/Pd. The surface area and size of nZVI/Pd were close to that of nZVI.

3.2 Degradation of BDE209 by microscale, nanoscale ZVI and nanoscale ZVI/Pd

The highest rate of BDE209 reduction was by the synthesized nZVI/Pd particles (Fig. 3). Approximately 90% of BDE209 was removed by nZVI/Pd particles within 80 min, whereas 25% of BDE209 was degraded by nZVI particles. Lower degradation rate was also observed in microscale ZVI treatment. The debromination of BDE209 fits pseudo-first-order kinetics. The degradation rate constants (k_{obs}) for nZVI/Pd and nZVI treatments were 0.0282 min^{-1} and 0.0036 min^{-1} respectively. The degradation rate constant of nZVI/Pd was about 8 times higher that of nZVI treatment.

3.3 Effect of pH on the removal of BDE209

Water pH appears to substantially influence the BDE209

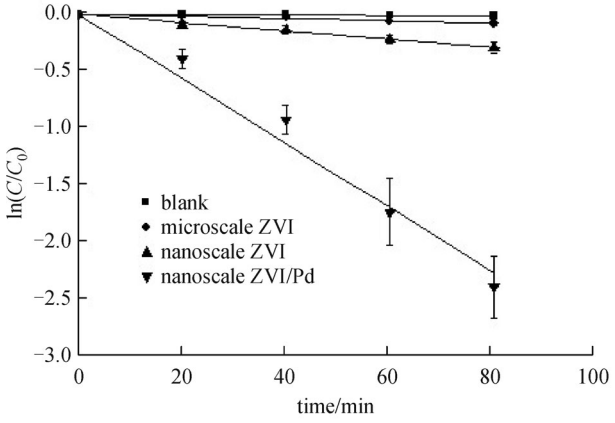

Fig. 3 Removal kinetics of BDE209 by microscale, nanoscale ZVI and nanoscale ZVI/Pd with initial pH of 5.0

degradation (Fig. 4). In the treatments with the initial pH of 5.0, 7.0, 8.0 and 9.0, the degradation rate constants (k_{obs}) were 0.026, 0.0085, 0.0053 and 0.0038 min^{-1}, respectively. The k_{obs} in the treatment with initial pH at 9.0 was more than 6.8 × higher than that under pH 5.0. The logarithm of the degradation rate constant had a linear relationship with initial pH ($r^2 = 0.989$):

$$\log k_{obs} = -0.2121\text{pH} - 0.5496, \quad (2)$$

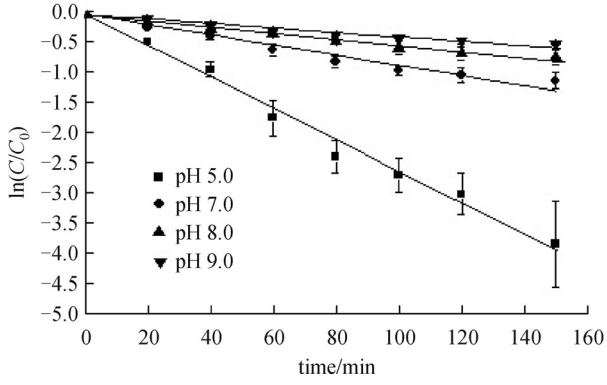

Fig. 4 Removal kinetics of BDE209 at pH 5.0, 7.0, 8.0 and 9.0 using Fe/Pd bimetallic nanoparticles

3.4 Degradation pathways

The BDE209 almost disappeared in the treatments within 150 min, resulting in many lower-brominated intermediates (Fig. 5). The degradation pathway of BDE209 was proposed in Fig. 6. In the first step, BDE209 was debrominated to the *non*-BDEs including BDE206, BDE207 and BDE208. BDE209 was debrominated by *ortho* substitution, *meta* substitution and *para* substitution to BDE206, BDE207 and BDE208. All these *non*-BDEs intermediates were identified (Fig. 5), confirming the removal of the first Br atom from BDE209. In the second step, *non*-BDEs were debrominated to the *octa*-BDEs. BDE206 was debrominated by *meta* substitution to BDE203, by *para* substitution to BDE198. BDE207 was debrominated by *meta* substitution to BDE197, by *ortho* substitution to BDE196. BDE208 was debrominated by *meta* substitution to BDE202, by *para* substitution to BDE201. These reactions have been confirmed by the identification of *octa*-BDEs intermediates. BDE196 and BDE197 were based on previous reports [24]. BDE198 was not observed, probably due to its co-eluting with BDE203 [25]. For this reason, peak of BDE203 also refers to BDE198. Based on the lack of bromine at both *para* positions, it was believed that the earliest eluting *octa*-BDE on commonly used nonpolar GC columns was BDE202 [25]. Since BDE201 was more stable than BDE200, it is reasonable to consider that the second *octa*-BDE peak in Fig. 5 is BDE201.

In the third step, *octa*-BDEs were debrominated to the *hepta*-BDEs. BDE203 debromination produced BDE181, 183 and 190 by *meta* and *ortho* substitution. BDE196, 197 were debrominated to BDE183 by *ortho* and *meta* substitution. BDE190, BDE183 and BDE181 were identified based on the standard solutions. In the fourth step, *hepta*-BDEs-BDEs was debrominated to the *hexa*-BDE. BDE181 and 190 were debrominated by *ortho* and *meta* substitution to BDE166. BDE183 was debrominated to BDE138 and 153 by *ortho* substitution, and to BDE154 by *para* substitution. Several major *hexa*-BDE congeners were formed. Among them, BDEs153, 154, 138 and 166 were identified based on the standard solutions.

In the fifth step, *hexa*-BDEs was debrominated to *penta*-BDEs. BDE166 substituted *para* bromine, producing BDE116. BDE138 was debrominated to BDE99 and 85 by *para* and *meta* substitution respectively. BDE153 substituted *meta* bromine, producing BDE99. BDE154 was debrominated to BDE100 and 119 by *meta* and *ortho* substitution respectively. Formation of *penta*-BDEs was also observed. BDE85, BDE116, BDE99, BDE119, and BDE100 were identified as *penta*-BDEs based on the standard solutions.

In the sixth step, *penta*-BDEs was debrominated to *tetra*-BDEs. BDE99 and 119 substituted *ortho* bromine, producing BDE66. BDE85, BDE99 and BDE100 were debrominated to BDE47 through *meta* and *ortho* substitution. *Tetra*-BDEs were produced with a number of congeners. *Tetra*-BDEs including BDE47 and BDE66 were identified based on the standard solutions.

In the seventh step, *tetra*-BDEs were debrominated to the *tir*-BDEs. BDE47 substituted *ortho* bromine, producing BDE28. BDE66 was debrominated to BDE33 and 37 by para and ortho substitution. BDE28/33, BDE37 were identified based on the standard solutions.

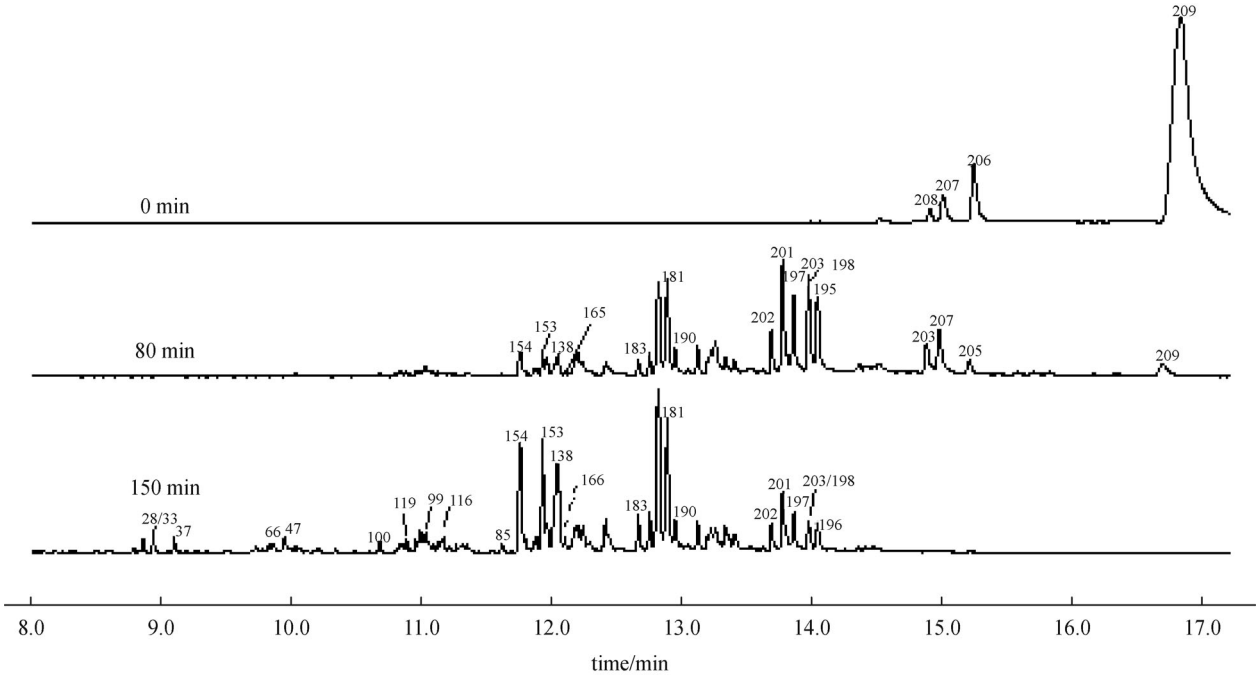

Fig. 5 GC-MS chromatogram of BDE209 and the degradation intermediates at different reaction times

4 Discussion

Removal of BDE209 in pure water using synthesized bimetallic NZVI/Pd was investigated. Rapid removal of BDE209 was observed, similar to the results from the acetone/water system [19]. The removal efficiency of BDE209 in the presence of Pd was more than 3.5 times higher than that without Pd, indicating the engagement of Pd (presumably as a catalyst) in the degradation. This result also agreed with other reports in which rapid dehalogenation occurred in the presence of catalyst Pd [16,17,19]. In addition to potential catalysis by Pd, the large surface area of nanoparticles is also expected to contribute to the removal of PBDEs [28]. In this study, approximately 10% of BDE209 could be extracted from both water and nZVI/Pd solid, suggesting that catalytic degradation instead of adsorption played a more important role. Previous studies show that Pd doping to nZVI surface could greatly affect the overall reaction through the facilitated oxidation of nZVI and Pd-meditated hydrogenation [29,30]. In the presence of iron, the corrosion of Fe^0 occurs under anaerobic conditions according to Eq. (3):

$$Fe^0 + 2H_2O \rightarrow Fe^{2+} + H_2 + 2OH^- \quad (3)$$

Based on this, there are three potential reductants (Fe^0, Fe^{2+}, H_2) in the Fe^0-H_2O system [31] that may contribute to the dehalogenation of BDE209 (Eqs.(4)–(6)).

$$Fe^0 + RBr_n + H \rightarrow Fe^{2+} + RBr_{n-1}H + Br^- \quad (4)$$

$$2Fe^{2+} + RBr_n + H^+ \rightarrow 2Fe^{3+} + RBr_{n-1}H + Br^- \quad (5)$$

$$H_2 + RBr_n \xrightarrow{Pd} RBr_{n-1}H + Br^- + H \quad (6)$$

However, the reactions are quite slow when Fe^0 or Fe^{2+} serves as the reductant [32–34]. Hydrogen (H_2) can only be used efficiently for the debromination of BDE209 via hydrodebromination in the presence of Pd [16,17,19]. In this process, H_2 is adsorbed by Pd (catalyst) and dissociated into atomic H to join in the debromination of BDE209 in the NZVI/Pd. The relatively high degradation efficiency of BDE209 in the presence of nZVI/Pd suggests that the main reductant for the dehalogenation of BDE209 in pure water was H_2, indicating that hydrodebromination is likely the main process in the degradation of BDE209.

The logarithm of the degradation rate constant has a linear relationship with initial pH of the reacting system, which was similar to the decabrominated dephenyl ether in the presence of nZVI [28]. The increase in water pH led to a decrease in the degradation efficiency of BDE209, indicating that acidic conditions were more favorable for the degradation of BDE209 [28]. More hydrogen could be produced under acidic conditions during the corrosion reaction of iron [29,30], which subsequently enhanced the degradation of BDE209. Additionally, the precipitation of metal hydroxides and metal carbonates on the surface of iron and Pd/Fe under high pH conditions may also decrease the corrosion (oxidation) of Fe, which subsequently jeopardized the degradation of BDE209.

The debromination of PBDEs by nZVI/Pd in pure water

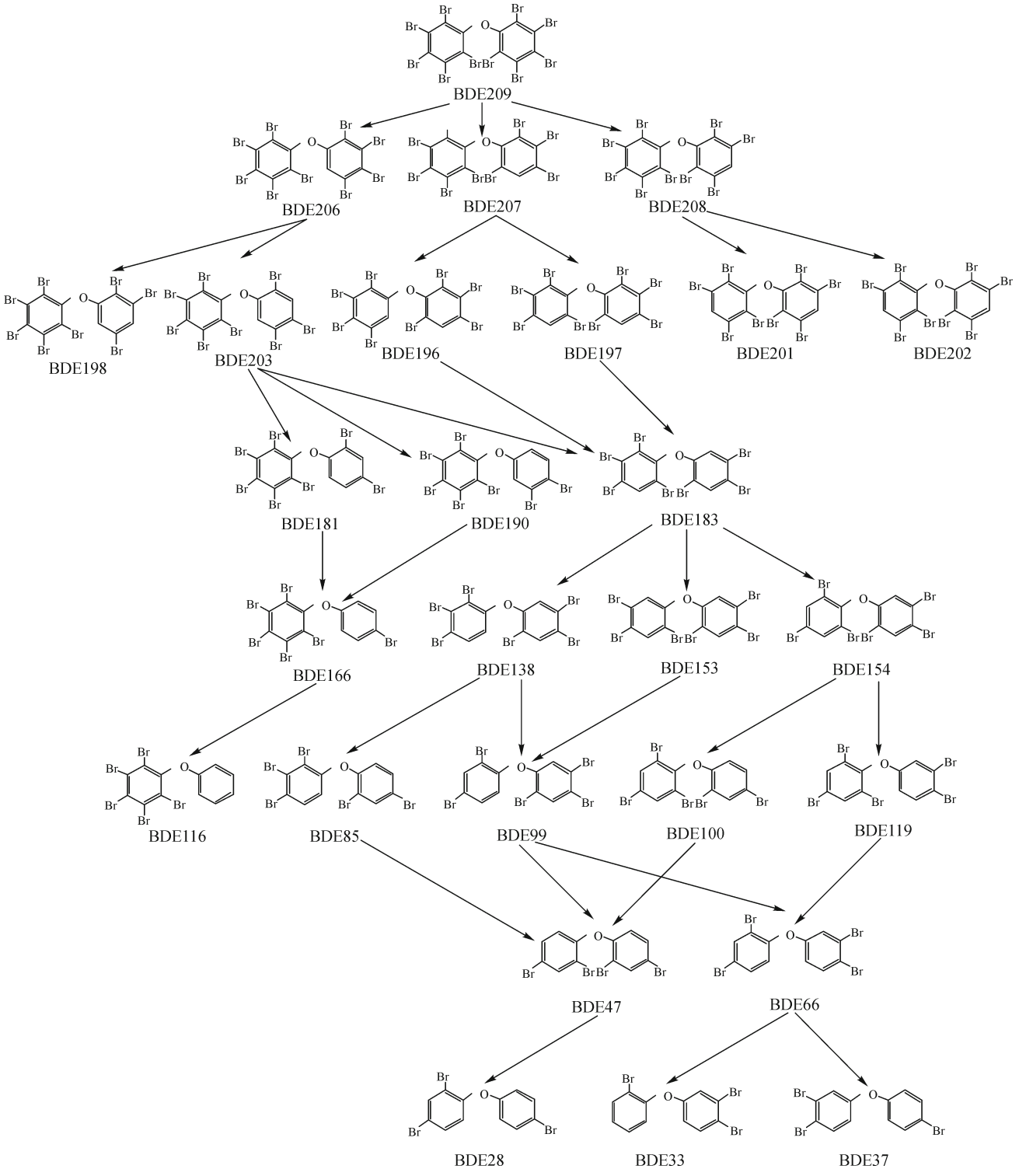

Fig. 6 Proposed pathway for the degradation of BDE209 in pure water in the presence of Fe/Pd bimetallic nanoparticles

system is a serial reaction, from *n*-BDE to (*n*–1)-BDE, which is similar to previous studies on stepwise dehalogenation of by ZVI [9,19]. Fang et al. [9] reported that stepwise dehalogenation was dominant when BDE209 was in contact with nZVI/Pd. During this study of BDE209 degradation by Fe/Pd bimetallic nanoparticle, previously reported intermediates such as *non*-BDEs (BDE206, BDE207, BDE208), *octa*-BDEs (BDE198, BDE203, BDE196, BDE197, BDE201, and BDE202), *hepta*-BDE (BDE181), *hexa*-BDEs (BDE166, and BDE138), *penta*-

BDEs (BDE116, BDE85, and BDE119), *tetra*-BDEs (BDE66), *tir*-BDEs (BDE33 and BDE37) were not observed [19], suggesting that degradation pathways of BDE209 in pure water system might be different from that in organic solvent/water system. Lower brominated intermediates appeared to accumulate in the pure water system while products with less bromines might be rapidly degraded in organic solvent/water [19,28]. Further investigation is needed to elucidate the differences between the BDE209 degradation pathways in pure water system and organic solvent/water system.

5 Conclusions

This paper investigated the removal of BDE209 in pure water using synthesized bimetallic NZVI/Pd. Rapid removal of BDE209 was observed, and the degradation appeared to follow a pseudo-first-order kinetics. The removal efficiency was significantly higher than that in microscale ZVI or nZVI treatments, indicating the advantage of Fe-based bimetallic nanoparticles in the removal of PBDEs. Higher removal efficiency under more acidic conditions was observed. The findings may offer a new measure for PBDEs removal using Fe/Pd bimetallic nanoparticles.

Acknowledgements This work is financially supported by National Science and Technology Major Projects of Water Pollution Control and Management of China (No. 2014ZX07206001).

References

1. Ahn M Y, Filley T R, Jafvert C T, Nies L, Hua I, Bezares-Cruz J. Photodegradation of decabromodiphenyl ether adsorbed onto clay minerals, metal oxides, and sediment. Environmental Science & Technology, 2006, 40(1): 215–220
2. Darnerud P O, Eriksen G S, Jóhannesson T, Larsen P B, Viluksela M. Polybrominated diphenyl ethers: occurrence, dietary exposure, and toxicology. Environmental Health Perspectives, 2001, 109(s1 Suppl 1): 49–68
3. Covaci A, Voorspoels S, de Boer J. Determination of brominated flame retardants, with emphasis on polybrominated diphenyl ethers (PBDEs) in environmental and human samples—a review. Environment International, 2003, 29(6): 735–756
4. Watkins D J, McClean M D, Fraser A J, Weinberg J, Stapleton H M, Sjödin A, Webster T F. Exposure to PBDEs in the office environment: evaluating the relationships between dust, handwipes, and serum. Environmental Health Perspectives, 2011, 119(9): 1247–1252
5. Ghosh U, Zimmerman J R, Luthy R G. PCB and PAH speciation among particle types in contaminated harbor sediments and effects on PAH bioavailability. Environmental Science & Technology, 2003, 37(10): 2209–2217
6. Ciparis S, Hale R C. Bioavailability of polybrominated diphenyl ether flame retardants in biosolids and spiked sediment to the aquatic oligochaete, Lumbriculus variegatus. Environmental Toxicology and Chemistry / SETAC, 2005, 24(4): 916–925
7. Murai S, Sonoda N, Tsutsumi S. Redox reaction of tetrahydrofuran hydroperoxide. Bulletin of the Chemical Society of Japan, 1963, 36 (5): 527–530
8. La Guardia M J, Hale R C, Harvey E. Detailed polybrominated diphenyl ether (PBDE) congener composition of the widely used penta-, octa-, and deca-PBDE technical flame-retardant mixtures. Environmental Science & Technology, 2006, 40(20): 6247–6254
9. Fang Z, Qiu X, Chen J, Qiu X. Debromination of polybrominated diphenyl ethers by Ni/Fe bimetallic nanoparticles: influencing factors, kinetics, and mechanism. Journal of Hazardous Materials, 2011, 185(2–3): 958–969
10. Zhuang Y, Ahn S, Luthy R G. Debromination of polybrominated diphenyl ethers by nanoscale zero-valent iron: pathways, kinetics, and reactivity. Environmental Science & Technology, 2010, 44(21): 8236–8242
11. Wang C B, Zhang W X. Synthesizing nanoscale iron particles for rapid and complete dechlorination of TCE and PCBs. Environmental Science & Technology, 1997, 31(7): 2154–2156
12. Fang Z, Qiu X, Chen J, Qiu X. Degradation of the polybrominated diphenyl ethers by nanoscale zero-valent metallic particles prepared from steel pickling waste liquor. Desalination, 2011, 267(1): 34–41
13. Qiu X, Fang Z, Liang B, Gu F, Xu Z. Degradation of decabromodiphenyl ether by nano zero-valent iron immobilized in mesoporous silica microspheres. Journal of Hazardous Materials, 2011, 193(15): 70–81
14. Xie Y, Fang Z, Cheng W, Tsang P E, Zhao D. Remediation of polybrominated diphenyl ethers in soil using Ni/Fe bimetallic nanoparticles: influencing factors, kinetics and mechanism. Science of the Total Environment, 2014, 485–486: 363–370
15. Kim E J, Kim J H, Kim J H, Bokare V, Chang Y S. Predicting reductive debromination of polybrominated diphenyl ethers by nanoscale zerovalent iron and its implications for environmental risk assessment. Science of the Total Environment, 2014, 470–471: 1553–1557
16. Wang X, Chen C, Liu H, Ma J. Characterization and evaluation of catalytic dechlorination activity of Pd/Fe bimetallic nanoparticles. Industrial & Engineering Chemistry Research, 2008, 47(22): 8645–8651
17. Wang X, Chen C, Chang Y, Liu H. Dechlorination of chlorinated methanes by Pd/Fe bimetallic nanoparticles. Journal of Hazardous Materials, 2009, 161(2–3): 815–823
18. Bokare A D, Chikate R C, Rode C V, Paknikar K M. Iron-nickel bimetallic nanoparticles for reductive degradation of azo dye orange G in aqueous solution. Applied Catalysis B: Environmental, 2008, 79(3): 270–278
19. Zhuang Y, Jin L, Luthy R G. Kinetics and pathways for the debromination of polybrominated diphenyl ethers by bimetallic and nanoscale zerovalent iron: effects of particle properties and catalyst. Chemosphere, 2012, 89(4): 426–432
20. Shih Y, Hsu C, Su Y. Reduction of hexachlorobenzene by nanoscale zero-valent iron: kinetics, pH effect, and degradation mechanism. Separation and Purification Technology, 2011, 76(3): 268–274
21. Chen X, Clark II C J. Modeling the effects of methanol on iron

dechlorination of a complex chlorinated NAPL. Journal of Hazardous Materials, 2009, 164(2–3): 565–570

22. Fang Z Q, Qiu X H, Chen J H, Qiu X Q. Degradation of the polybrominated diphenyl ethers by nanoscale zero-valent metallic particles prepared from steel pickling waste liquor. Desalination, 2011, 267(1): 34–41
23. Wang Y, Li A, Liu H, Zhang Q, Ma W, Song W, Jiang G. Development of quantitative structure gas chromatographic relative retention time models on seven stationary phases for 209 polybrominated diphenyl ether congeners. Journal of Chromatography A, 2006, 1103(2): 314–328
24. Bezares-Cruz J, Jafvert C T, Hua I. Solar photodecomposition of decabromodiphenyl ether: products and quantum yield. Environmental Science & Technology, 2004, 38(15): 4149–4156
25. Gerecke A C, Hartmann P C, Heeb N V, Kohler H P, Giger W, Schmid P, Zennegg M, Kohler M. Anaerobic degradation of decabromodiphenyl ether. Environmental Science & Technology, 2005, 39(4): 1078–1083
26. Xu H Y, Zou J W, Yu Q S, Wang Y H, Zhang J Y, Jin H X. QSPR/QSAR models for prediction of the physicochemical properties and biological activity of polybrominated diphenyl ethers. Chemosphere, 2007, 66(10): 1998–2010
27. Li A, Tai C, Zhao Z, Wang Y, Zhang Q, Jiang G, Hu J. Debromination of decabrominated diphenyl ether by resin-bound iron nanoparticles. Environmental Science & Technology, 2007, 41 (19): 6841–6846
28. Shih Y H, Tai Y T. Reaction of decabrominated diphenyl ether by zerovalent iron nanoparticles. Chemosphere, 2010, 78(10): 1200–1206
29. Grittini C, Malcomson M, Fernando Q, Korte N. Rapid dechlorination of polychlorinated biphenyls on the surface of a Pd/Fe bimetallic system. Environmental Science & Technology, 1995, 29(11): 2898–2900
30. Agarwal S, Al-Abed S R, Dionysiou D D. Enhanced corrosion-based Pd/Mg bimetallic systems for dechlorination of PCBs. Environmental Science & Technology, 2007, 41(10): 3722–3727
31. Matheson L J, Tratnyek P G. Reductive dehalogenation of chlorinated methanes by iron metal. Environmental Science & Technology, 1994, 28(12): 2045–2053
32. Doong R A, Wu S C. Reductive dechlorination of chlorinated hydrocarbons in solutions containing ferrous and sulfide ions. Chemosphere, 1992, 24(8): 1063–1075
33. Klečka G M, Gonsior S J. Reductive dechlorination of chlorinated methanes and ethanes by reduced iron (II) porphyrins. Chemosphere, 1984, 13(3): 391–402
34. O'carroll D, Sleep B, Krol M, Boparai H, Kocur C. Nanoscale zero valent iron and bimetallic particles for contaminated site remediation. Advances in Water Resources, 2013, 51: 104–122